Philosophical Magazine,
Vol. 85, Nos. 33–35, 21 Nov.–11 Dec. 2005, 4055–4065

Taylor & Francis
Taylor & Francis Group

Quasicontinuum modelling of short-wave instabilities in crystal lattices

L. TRUSKINOVSKY† and A. VAINCHTEIN*‡

†Laboratoire de Mechanique des Solides, CNRS-UMR 7649, Ecole Polytechnique, Palaiseau, 91128, France
‡Department of Mathematics, University of Pittsburgh, Pittsburgh, PA 15260, USA

(*Received 12 May 2004; in final form 22 November 2004*)

We propose a hybrid quasicontinuum model which captures both long and short-wave instabilities of crystal lattices and combines the advantages of weakly non-local (higher gradient) and strongly non-local (integral) continuum models. To illustrate the idea, we study the simplest one-dimensional lattice exhibiting commensurate and incommensurate short-wave instabilities. We explicitly compute stability limits of the homogeneous states using both discrete and quasicontinuum models. The new quasicontinuum approximation is shown to be capable of reproducing a detailed structure of the discrete stability diagram.

1. Introduction

Lattice instabilities are responsible for various transformations of crystal structures. Macroscopic or long-wave instabilities give rise to martensitic phase transformations, which proceed through the formation of finite-size domains of the new phase [1, 2]. Microscopic or short-wave instabilities lead to the formation of multi-lattices and modulated ''tweed'' patterns [2–4]. Both micro- and macroinstabilities are detectable in the phonon dispersion spectra. The loss of stability takes place when the minimum of the dispersion curve touches the zero frequency level [5–7]. Macroscopic instabilities correspond to infinitely long waves and can be linked to the softening of the appropriate combinations of macroscopic elastic moduli. Typical microscopic instabilities occur at finite wave lengths associated with special points in the Brillouin zone corresponding to modulations commensurate with the lattice. Less frequent microinstabilities with the generic wave vectors give rise to incommensurate phases [8].

The classical continuum description of lattice instabilities is provided by the Landau theory. When the unstable wave vector is equal to zero, the order parameter can be chosen to coincide with a component of the macroscopic strain (see, for example, Fadda *et al.* [9]). If the unstable wave vector is different from zero, the macroscopic order parameter can be identified with the amplitude of an unstable normal mode (see, for example, Cao and Barsch [10]). The resulting coarse-grained

*Corresponding author. Email: aav4@pitt.edu

Philosophical Magazine
ISSN 1478–6435 print/ISSN 1478–6443 online © 2005 Taylor & Francis
http://www.tandf.co.uk/journals
DOI: 10.1080/14786430500363270

description remains adequate until external length scales become comparable with the lattice spacing, as in the cases of ultra-thin layers, boundaries with singularities or strongly interacting defects.

To preserve the fine structure of the elastic fields in the continuum setting we propose a new quasicontinuum model which captures both long and short-wave instabilities associated with the acoustic branch of the phonon spectrum. The model is obtained by a long-wave expansion of the lattice energy and it shares with the discrete model the property that strain is the only order parameter. To make the truncated gradient expansion well-posed, we extend the polynomial dispersion relation by zero outside the first Brillouin zone. The model therefore restricts modulations in the physical space to length scales larger than lattice spacing. The suppression of the gradient model outside the Brillouin zone allows one to avoid the unphysical small-scale instabilities; a similar hard cut-off procedure is routinely used in coarse-grained continuum field theories [11]. As we show, the cut-off makes the gradient model equivalent to a fully non-local model with a slowly decaying oscillatory kernel.

To illustrate the idea, we consider a one-dimenstional lattice involving interactions of up to third nearest neighbours which can be either of ferromagnetic or antiferromagnetic type. The discrete model is shown to generate both commensurate and incommensurate short-wave instabilities (see, for example, Houchmandzadeh *et al.* [12] and Janssen and Tjon [13]). We show that the quasicontinuum model captures all unstable modes exhibited by the discrete model and provides good quantitative bounds for the instability thresholds.

2. Discrete model

Consider an infinite chain of interacting particles with the total energy

$$W = \varepsilon \sum_{n=-\infty}^{\infty} \sum_{p=1}^{q} p\phi_p\left(\frac{u_{n+p} - u_n}{p\varepsilon}\right). \tag{1}$$

Here $\phi_p(w)$ is the energy density of an effective spring with reference length $p\varepsilon$ (representing interaction of pth nearest neighbours) and $u_n(t)$ is the displacement of nth particle. The equilibria in this system satisfy the following infinite system of difference equations:

$$\sum_{p=1}^{q} \left[\phi_p'\left(\frac{u_{n+p} - u_n}{p\varepsilon}\right) - \phi_p'\left(\frac{u_n - u_{n-p}}{p\varepsilon}\right)\right] = 0. \tag{2}$$

To access stability of a homogeneous equilibrium state $u_n^0 = n\varepsilon w$, where w is the average strain, we need to introduce perturbations $v_n = u_n - u_n^0$ and study the positive definiteness of the quadratic part of the energy expansion. This leads to the following eigenvalue problem:

$$-\omega^2 v_n = \sum_{p=1}^{q} K_p\left(v_{n+p} - 2v_n + v_{n-p}\right), \tag{3}$$

where $K_p = \phi_p''(w)/p$ and ω^2 is the square of the characteristic frequency. By representing the normal modes (phonons) in the form $v_n = \exp(ink)$, where k is a real wave number, we obtain the dispersion relation

$$\omega^2(k) = 4\sum_{p=1}^{q} K_p \sin^2\frac{pk}{2}. \tag{4}$$

By reflectional symmetry and periodicity it suffices to consider the wave numbers in the interval $0 \le k \le \pi$ (Brillouin zone). A uniform deformation is then stable if and only if $\omega^2(k) > 0$ for all $k \in (0, \pi]$. This condition is the far reaching generalization of the Legendre–Hadamard condition of strong ellipticity in continuum elasticity [14].

One can obtain some immediate necessary conditions for stability by requiring that

$$\frac{d^2\omega^2(0)}{dk^2} > 0 \quad \text{and} \quad \omega^2(\pi) > 0.$$

The first condition, written as

$$E = \sum_{p=1}^{q} p^2 K_p > 0, \tag{5}$$

means physically that the effective elastic modulus along the homogeneous branch of equilibria is positive; the corresponding eigenmode, $v_n = 1$, is infinitely long wave. The second condition,

$$\sum_{k=1,\, k\,\text{odd}}^{q} K_p > 0, \tag{6}$$

is less transparent: the corresponding unstable eigenmode $v_n = (-1)^n$ is microscopic, commensurate and has the smallest possible wave length.

To characterize the complete set of stability conditions (necessary and sufficient) explicitly, we need to specify the number of interactions. One can show that the first generic case is $q = 3$, when nearest (NN), next to nearest (NNN) and next to next to nearest (NNNN) neighbours interact. The corresponding dispersion relation reads

$$\omega^2(k) = 4\sin^2\frac{k}{2}\left(K_1 + 4K_2 + 9K_3 - 4(K_2 + 6K_3)\sin^2\frac{k}{2} + 16K_3\sin^4\frac{k}{2}\right). \tag{7}$$

A straightforward analysis of the positive definiteness of the right hand side produces the following necessary and sufficient conditions of stability:

$$\begin{aligned} &K_1 + 4K_2 + 9K_3 > 0 \\ &K_1 + K_3 > 0 \\ &K_2^2 < 4K_3(K_1 + K_2) \quad \text{if} \quad -6 < \frac{K_2}{K_3} < 2. \end{aligned} \tag{8}$$

The first two of these conditions have been already obtained as necessary (see equalities (5)–(6)) and can be identified with macroinstabilities ($k=0$) and commensurate microinstabilities ($k=\pi$), respectively. The third condition in (8) is associated with the incommensurate mode $0<k=2\arcsin\sqrt{(K_2+6K_3)/(8K_3)}<\pi$. The full stability diagram in the plane of the non-dimensional parameters

$$\alpha=\frac{K_2}{K_1},\qquad \beta=\frac{K_3}{K_1} \tag{9}$$

is presented in figure 1 for $K_1>0$ and figure 2 for $K_1<0$.

To relate the microscopic stability limits with macroscopic stress–strain relation, consider a family of homogeneous configurations $u_n=wn\varepsilon$ parametrized by the strain w. Assume that all three interactions (NN, NNN and NNNN) are governed by the Morse potentials

$$U_p(r)=\frac{\mu_p\varepsilon}{2\gamma_p^2}\left(1-\exp\left[-\gamma_p\left(\frac{r}{\varepsilon}-1\right)\right]\right)^2,\quad 1\le p\le 3. \tag{10}$$

The energy density associated with pth interaction in the homogeneous state is

$$\phi_p(w)=U_p(p\varepsilon(w+1))/(p\varepsilon); \tag{11}$$

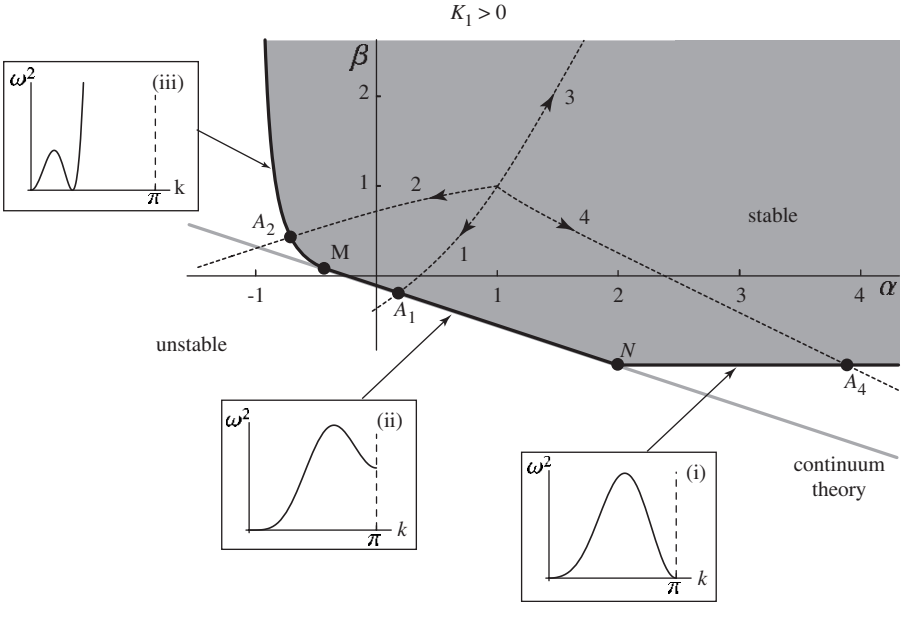

Figure 1. Stability diagram for the discrete model with $q=3$ and $K_1>0$. Regions of stability are shown in grey. Dispersion relations corresponding to different modes of stability loss are shown in inserts. Stability boundaries: (i) commensurate microinstability, $\beta=-1$ (to the right of N); (ii) macroinstability, $1+4\alpha+9\beta=0$ (between N and M); (iii) incommensurate microinstability, $\alpha^2=4\beta(1+\alpha)$ (above M). Classical continuum stability boundary is given by the grey line, $1+4\alpha+9\beta=0$. Dashed lines with numbers indicate deformation paths: $\gamma_2=\gamma_3=1$ (path 1); $\gamma_2=1$, $\gamma_3=0.4$ (path 2); $\gamma_2=0.4$, $\gamma_3=0.2$ (path 3); $\gamma_2=\gamma_3=0.4$ (path 4). In all cases $\mu_1=\mu_2=\mu_3=\gamma_1=1$.

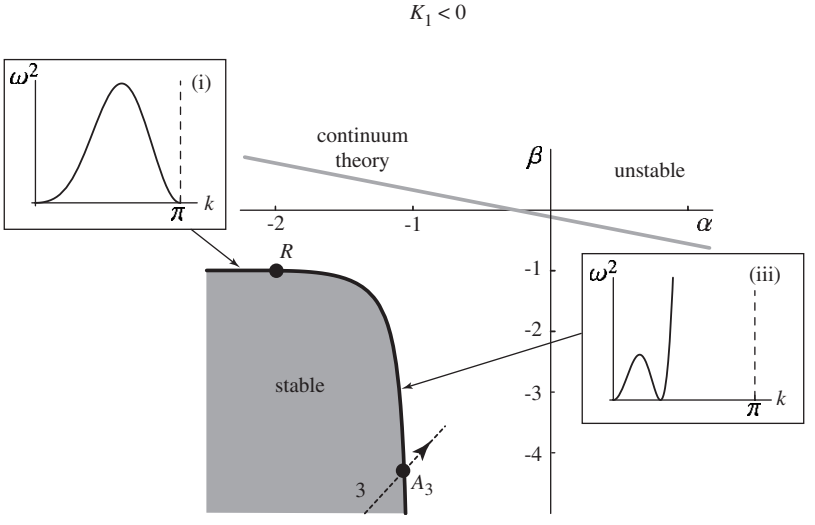

Figure 2. Stability diagram for the discrete model with $q = 3$ and $K_1 < 0$. Stability boundaries: (i) commensurate microinstability, $\beta = -1$ (to the left or R); (iii) incommensurate microinstability, $\alpha^2 = 4\beta(1+\alpha)$ (below R). Dashed line indicates deformation path 3 which is also shown in figure 1.

the elastic moduli are given by

$$K_p(w) = \mu_p \exp[-p\gamma_p w](2\exp[-p\gamma_p w] - 1), \quad 1 \le p \le 3. \tag{12}$$

Using equations (9) and (12), we can compute the strain dependence of the dimensionless parameters $\alpha(w)$ and $\beta(w)$. Depending on the choice of the microscopic parameters μ_p and γ_p, we obtain different paths in the α–β plane; each path starts in the stable region and eventually reaches the instability threshold. If the potentials are identical for NN, NNN and NNNN interactions ($\mu_1 = \mu_2 = \mu_3$, $\gamma_1 = \gamma_2 = \gamma_3$), the resulting homogeneous equilibrium branch (path 1 in figure 1) crosses the macroinstability boundary MN, activating the instability mode $\nu_n = 1$. The corresponding macroscopic stress–strain relation $\sigma(w)$ is shown in figure 3. In this case the bifurcation point A_1 corresponds to the failure of the Legendre–Hadamard conditions for the macroscopic energy ($\sigma'(w) = 0$).

Suppose next that the three considered interactions (NN, NNN and NNNN) are governed by different Morse potentials. For instance, we may assume that $U_1'(r) = U_2'(r)$ but that the force associated with the NNNN interaction $U_3'(r)$ decays at large r slower than $U_1'(r)$. If γ_3 is sufficiently smaller than $\gamma_1 = \gamma_2$, the corresponding equilibrium branch (path 2 in figure 1) crosses the incommensurate microinstability boundary. The stability is lost at point A_2 where $\sigma'(w) > 0$, i.e. *before* the macroscopic threshold.

Now suppose that $U_2'(r)$ decays slower than $U_1'(r)$ but faster than $U_3'(r)$ (e.g. $\gamma_1 = 1$, $\gamma_2 = 0.4$, $\gamma_3 = 0.2$). The corresponding equilibrium path 3 starts in the stable region where all three elastic moduli are positive (see figure 1). As w increases, $K_1(w)$ approaches zero faster than the other two moduli, so that α and β both tend to infinity. When K_1 changes sign, parameters α and β become infinite and the path re-emerges in the stable region with $K_1 < 0$ (figure 2). The failure of the

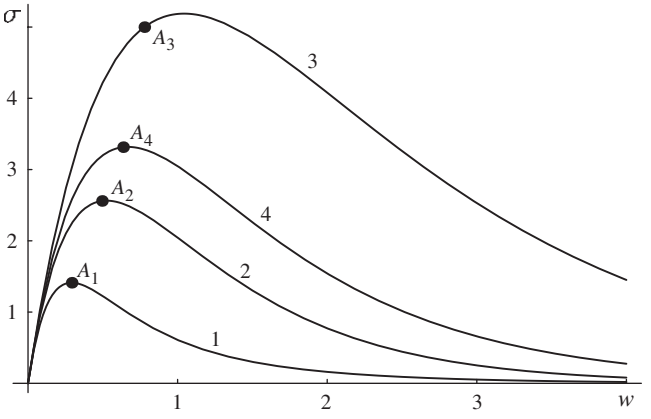

Figure 3. Stress–strain relations along the deformation paths shown in figures 1 and 2. Points A_i mark the loss of stability of the homogeneous deformation.

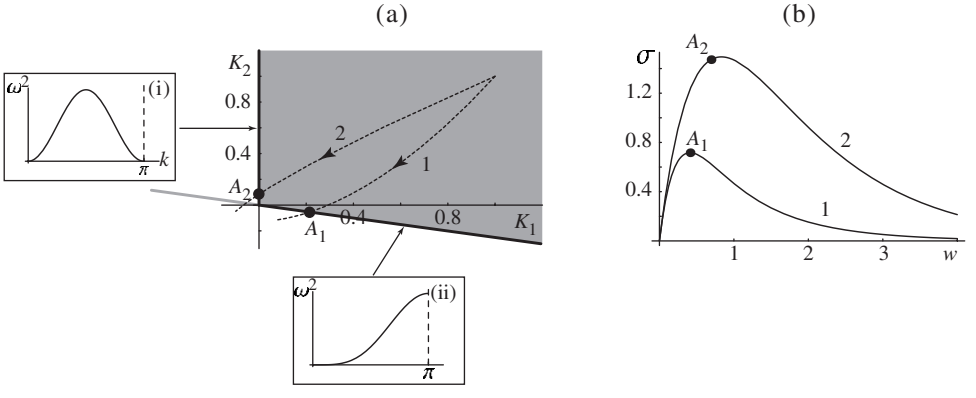

Figure 4. (a) Stability diagram for the discrete model with $q=2$. The trivial solution is stable in the grey area. Stability boundaries: (i) commensurate microinstability, $K_1=0$; (ii) macroinstability, $K_1+4K_2=0$. In the classical continuum model the trivial solution is stable above the grey line $K_1+4K_2=0$. The dotted curves show deformation paths: $\gamma_2=1$ (path 1) and $\gamma_2=0.4$ (path 2). In both cases $\mu_1=\mu_2=\gamma_1=1$. (b) The corresponding stress–strain curves.

homogeneous state at A_3 takes place via incommensurate microinstability before the macroinstability threshold.

Finally, assume that NNN and NNNN interactions potentials are identical and that the corresponding forces decay slower than $U_1'(r)$ ($\gamma_1 = 1, \gamma_2 = \gamma_3 = 0.4$). Then we obtained path 4 which crosses the commensurate microinstability boundary at point A_4 to the right of point N in figure 1. The corresponding microinstability again precedes the macroinstability (see figure 3).

In the special case when the only two interactions are NN and NNN ($q=2$, $K_3=0$), the stability conditions (8) reduce to $K_1+4K_2 > 0$, $K_1 > 0$ [15]; see the shaded region in figure 4a. In this case the microinstability is necessarily commensurate, and it takes place at $K_1=0$. As before, the path with identical potentials for NN and NNN interactions (path 1) leads to macroinstability. If $U_2'(r)$ decays slower than $U_1'(r)$, the instability becomes microscopic (see figure 4b).

3. Quasicontinuum approximation

A higher gradient quasicontinuun approximation of a lattice model is obtained by replacing the discrete dispersion relation equation (4) by the first few terms of its Taylor expansion around $k=0$ [16, 17]. To capture all three types of instabilities (long-wave, commensurate and incommensurate) exhibited by the discrete model with $q \geq 3$, it is necessary to consider a polynomial expansion of at least sixth order:

$$\omega^2(k) \approx k^2(E + A_1 k^2 + A_2 k^4), \tag{13}$$

where the Taylor coefficients are

$$\begin{aligned} E &= K_1 + 4K_2 + 9K_3 \\ A_1 &= -\frac{K_1 + 16K_2 + 81\,K_3}{12} \\ A_2 &= \frac{K_1 + 64K_2 + 729\,K_3}{360}. \end{aligned} \tag{14}$$

The quadratic part of the continuum energy function corresponding to equation (13) takes the form

$$W = \frac{1}{2}\int_{-\infty}^{\infty} [Eu_x^2 + A_1\varepsilon^2 u_{xx}^2 + A_2\varepsilon^4 u_{xxx}^2]\,dx. \tag{15}$$

To access stability of the homogeneous state in the continuum problem we need to solve the following eigenvalue problem:

$$-\omega^2 v = Ev_{xx} - A_1\varepsilon^2 v_{xxxx} + A_2\varepsilon^4 v_{xxxxxx}. \tag{16}$$

One can immediately see that if $A_2 < 0$ the energy is unbounded from below ($\omega^2(k) < 0$ for sufficiently large $|k|$). This short-wave instability is unphysical if the unstable wave length is shorter than the lattice spacing. To eliminate this possibility we can limit the class of perturbations by imposing a constraint $|k| \leq \pi$. This is achieved by replacing equation (13) with $\omega^2(k) = 0$ outside the first Brillouin zone (for $|k| > \pi$). The resulting dispersion relation with a short wave cut-off is compared in figure 5 with the dispersion relation for the *exact* quasicontinuum model [18] obtained by replacing discrete dispersion by zero at $|k| > \pi$.

Despite its appearance, the proposed higher gradient approximation with a cut-off is essentially a continuum model with long-range spatial memory. Indeed, if we compute inverse Fourier transform of the truncated dispersion relation (13), we obtain the integral model

$$W = \int_{-\infty}^{\infty}\int_{-\infty}^{\infty} \Phi(x-\xi)u(x,t)u(\xi,t)\,dx\,d\xi \tag{17}$$

with the kernel

$$\begin{aligned} \Phi(x) = \frac{1}{\pi x^7}[&2\pi x((E + 2A_1\pi^2 + 3A_2\pi^4)x^4 - 12(A_1 + 5A_2\pi^2)x^2 + 360A_2)\cos\pi x \\ &+ (\pi^2 x^6(E + A_1\pi^2 + A_2\pi^4) + 2(E + 6A_1\pi^2 + 15A_2\pi^4)x^4 \\ &+ 24(A_1 + 15A_2\pi^2)x^2 - 720A_2)\sin\pi x]. \end{aligned} \tag{18}$$

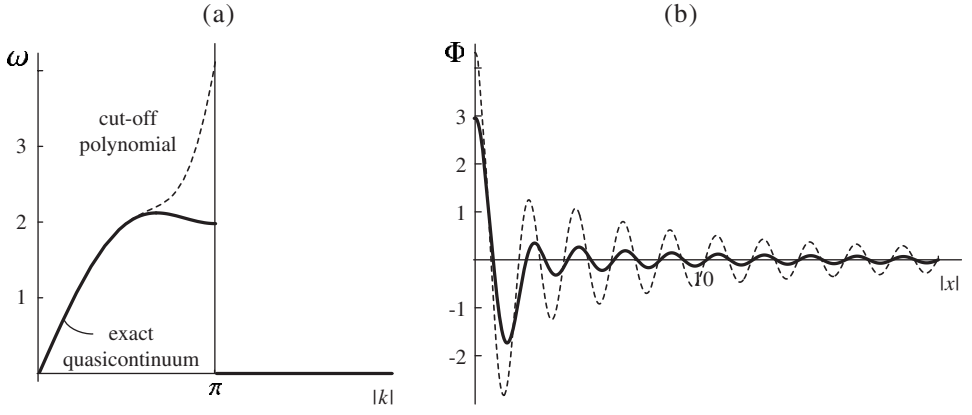

Figure 5. (a) Dispersion relations $\omega(k)$ for the exact quasicontinuum model (thick solid line) and the cut-off polynomial approximation (dashed). (b) The kernels $\Phi(x)$ of the exact quasicontinuum (solid) and cut-off polynomial (dashed) non-local models in physical space. Parameters: $K_1 = 1$, $K_2 = 5$, $K_3 = -0.02$.

Meanwhile, the exact quasicontinuum model has the kernel (see, for example, Kunin [18])

$$\Phi_D(x) = \frac{4\sin \pi x}{\pi x}\left(K_1 \frac{x^2 - 1/2}{x^2 - 1} - \frac{2K_2}{x^2 - 4} + K_3 \frac{x^2 - 9/2}{x^2 - 9}\right). \tag{19}$$

The two kernels are compared in figure 5b; one can see that the non-local interactions decay in both cases as a power of distance which is characteristic for the models with long-range interactions.

The proposed quasicontinuum model can be used to study stability of the homogeneous state. Following the same procedure as in the discrete case, we obtain the following necessary and sufficient conditions of stability:

$$\begin{aligned} &E > 0 \\ &E + A_1\pi^2 + A_2\pi^4 > 0 \\ &4A_2E - A_1^2 > 0 \quad \text{if} \quad 0 < -\frac{A_1}{2A_2} < \pi^2. \end{aligned} \tag{20}$$

The first condition, indicating macroinstability, coincides with the first inequality in (8). The second condition is the analog of the second inequality in (8), and the unstable mode is again $k = \pi$. The last inequality in (20) is analogous to the third condition of equation (8); its failure corresponds to incommensurate microinstability with the wave number

$$k = k^* = \sqrt{-\frac{A_1}{2A_2}}. \tag{21}$$

A combined stability diagram illustrating conditions (20) is presented in figure 6 where it is compared with the stability diagram for the discrete model.

Observe first that in the discrete and quasicontinuum models at $K_1 > 0$ the stability boundaries are tangent at point M where the unstable wave is infinitely long ($k = 0$).

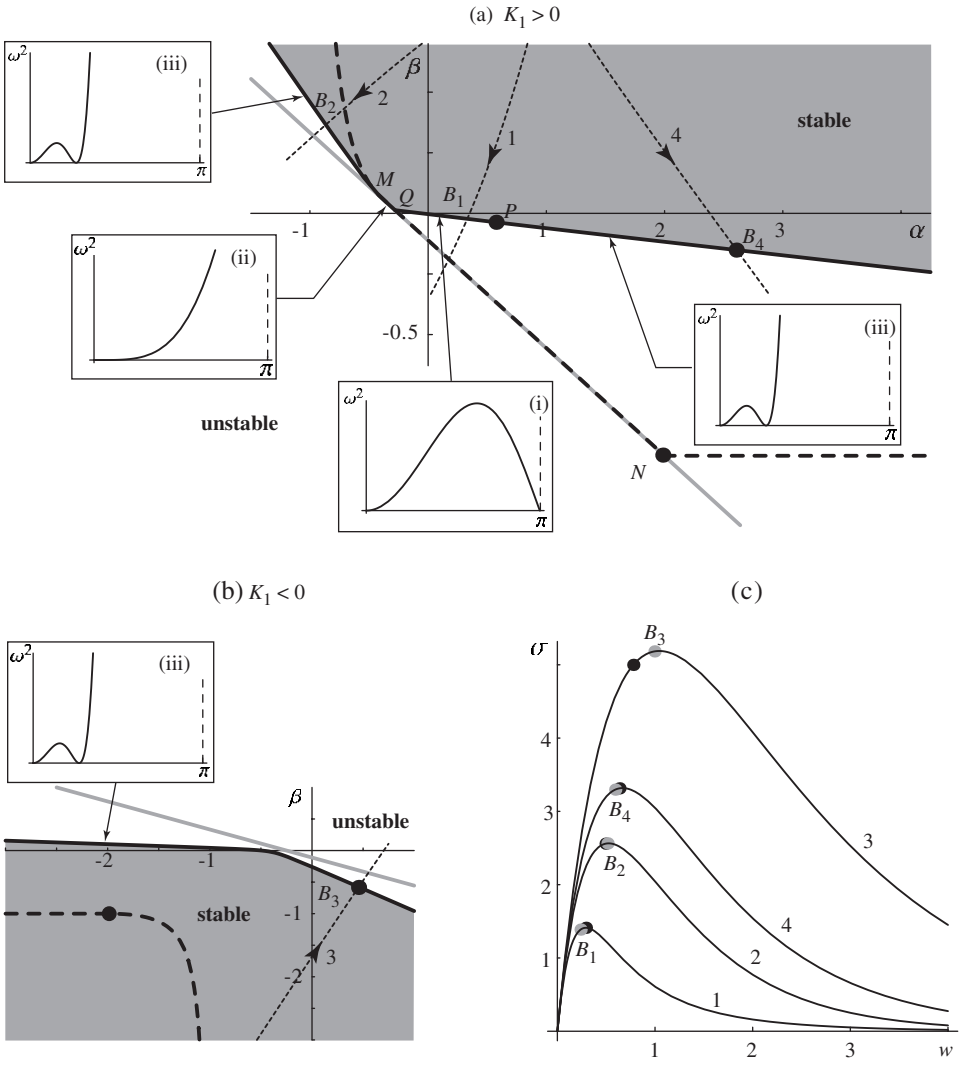

Figure 6. Stability diagram for the quasicontinuum polynomial model with the cut-off compared with the discrete stability diagram. Regions of stability are shown in grey, the corresponding graphs of $\omega^2(k)$ (dispersion relations) are shown in the inserts. Dashed curves indicate stability bounds for the discrete model. The two main diagrams correspond to the cases (a) $K_1 > 0$ and (b) $K_1 < 0$. Stability boundaries: (i) commensurate microinstability, $E + A_1\pi^2 + A_2\pi^4 = 0$ (PQ); (ii) macroinstability, $E = 0$ (MQ); (iii) incommensurate micro-instability, $4A_2E - A_1^2 = 0$ (above M, below P and entire boundary of $K_1 < 0$ stability region in (b)). Classical continuum model predicts stability above the grey line in (a) and below it in (b). In (c) we present stress–strain relations along the deformation paths (the same as in figure 1) shown by the dotted curves in (a) and (b), with bifurcation points for quasicontinuum model shown by grey circles and for the discrete model by black circles.

Above point M the quasicontinuum model reproduces the main qualitative features of the discrete diagram. Between points M and $Q = (-4(\pi^2 - 3)/(13\pi^2 - 30), (\pi^2 - 6)/(3(13\pi^2 - 30))$ the instability mode is macroscopic in both models; this interval, however, is much shorter in the quasicontinuum model.

Between points Q and $P = (-(120 - 80\pi^2 + 3\pi^4)/(10(30 - 26\pi^2 + 3\pi^4)), -(30\pi^2 - \pi^4 - 90)/(45(30 - 26\pi^2 + 3\pi^4))$ the stability loss is via microscopic mode with $k = \pi$. Below P the instability mode is again incommensurate; such transition from commensurate to incommensurate instability is not observed in the discrete case. Overall, the quasicontinuum theory underestimates stability domains in the region $\{K_1 > 0,\ K_2 > 0,\ K_3 < 0\}$. This is due to the larger contribution of the oscillation-producing K_3 terms in the polynomial model compared to the discrete case.

At $K_1 < 0$ the quasicontinuum approximation has the opposite effect: it overestimates the stability of the homogeneous state. This is again caused by the very nature of the polynomial approximation: for positive K_2 and K_3 (which at $K_1 < 0$ result in negative α and β) the smoothening quadratic and quartic terms in the dispersion relation easily dominate the unstable contribution due to K_1. Notice also that while in the discrete case the boundary of the stable domain contains a segment corresponding to commensurate instability (which at point R becomes incommensurate), in the polynomial quasicontinuum model the whole instability boundary is due to incommensurate mode.

It is instructive to compare the instability mechanisms along the four deformation paths considered earlier for the discrete model with the predictions of the quasicontinuum models (see figure 6). Along path 1 the quasicontinuum approximation predicts a commensurate microinstability (at point B_1), whereas the discrete model predicts macroscopic instability. Both models predict incommensurate instability along paths 2 and 3, with stability failure somewhat delayed in the quasicontinuum model. Finally, path 4 is predicted to pass through microinstability boundary by both models; the mode of instability is, however, commensurate in the discrete case and incommensurate in the quasicontinuum approximation. The analysis of the relative position of the bifurcation points on the stress–strain curves, presented for both models in figure 6c, shows a reasonable quantitative agreement.

4. Conclusions

It has been long recognized that higher gradient approximations of lattice models generate in the continuum limit either unbounded or non-positive definite operators leading to ill-posed mathematical problems (see, for example, Christov *et al.* [19] and Rosenau [20]). To overcome this difficulty we propose to regularize such operators by restricting them to a finite sphere in the Fourier space. At short wavelengths the resulting quasicontinuum model effectively replaces partial differential equations by integral equations. The dual nature of such cut-off polynomial models may be used to design hybrid computational schemes filtering parasitic small-scale oscillations while taking full advantage of the availability of simple partial differential equations for slowly varying fields. As we showed, the new quasicontinuum model combines the analytical simplicity of the gradient models at long waves with the physically corrent description at small scales provided by models with long spatial memory. In particular, the approximation was shown to be sufficient to capture the whole spectrum of short-wave instabilities exhibited by the prototypical lattice model.

Acknowledgements

This work was supported by the NSF grants DMS-0102841 (L.T.) and DMS-0137634 (A.V.).

References

[1] M. Pitteri and G. Zanzotto, *Continuum Theories for Phase Transitions and Twinning in Crystals* (Chapman and Hall, London, 2004).
[2] P. Toledano and V. Dmitriev, *Reconstructive Phase Transitions: in Crystals and Quasicrystals* (World Scientific, Singapore, 1996).
[3] T. Castan, A. Planes and A. Saxena, Phys. Rev. B **67** 134113 (2003).
[4] S. Kartha, J. Krumhansl, J. Sethna, *et al.*, Phys. Rev. B **52** 803 (1995).
[5] X. Xuang, C. Bungaro, V. Godlevsky, *et al.*, Phys. Rev. B **65** 014108 (2002).
[6] D.C. Wallace, *Thermodynamics of Crystals* (Dover Publications, New York, 1998).
[7] N. Triantafyllidis and S. Bardenhagen, J. Mech. Phys. Solids **44** 1891 (1996).
[8] T. Janssen and A. Janner, Adv. Phys. **36** 519 (1987).
[9] G. Fadda, L. Truskinovsky and G. Zanzotto, Phys. Rev. B **66** 174107 (2002).
[10] W. Cao and G.R. Barsch, Phys. Rev. B **41** 4334 (1990).
[11] P.M. Chaikin and T.C. Lubensky, *Principles of Condensed Matter Physics* (Cambridge University Press, Cambridge, 2000).
[12] B. Houchmandzadeh, J. Lajzerowicz and E. Salje, J. Phys. Condensed Matter **4** 9779 (1992).
[13] T. Janssen and J. Tjon, Phys. Rev. B **25** 3767 (1982).
[14] R. Hill, J. Mech. Phys. Solids **10** 1 (1962).
[15] L. Truskinovsky and A. Vainchtein, J. Mech. Phys. Solids **52** 1421 (2004).
[16] G.R. Barsch and K. Krumhansl, Metall. Trans. A **19** 761 (1988).
[17] R.D. Mindlin, Int. J. Solids Struct. **1** 417 (1965).
[18] I.A. Kunin, *Elastic Media with Microstructure I: One-Dimensional Models* (Springer-Verlag, Berlin, 1982).
[19] C.I. Christov, G.A. Maugin and M.G. Velarde, Phys. Rev. E **54** 3621 (1996).
[20] P. Rosenau, Phys. Let. A **311** 39 (2003).